Supplemental Material for

Microscopy of hydrogen and hydrogen-vacancy defect structures on graphene devices

Dillon Wong, Yang Wang, Wuwei Jin, Hsin-Zon Tsai, Aaron Bostwick, Eli Rotenberg, Roland K. Kawakami, Alex Zettl, Arash A. Mostofi, Johannes Lischner, Michael F. Crommie

1. d*I*/d*V* spectra for triangular defects

Fig. S1 shows d*I*/*dV* spectroscopy acquired on a triangular defect for different values of the gate voltage V_g.

2. Density of states calculations for hydrogen defect structures

Fig. S2 shows the density of states (calculated via density functional theory (DFT)) for an ortho dimer, a para dimer, a monohydrogen-monovacancy, and a dihydrogen-monovacancy. There are two resonances flanking the Dirac point, but these resonances are at energies beyond those probed in d*I*/d*V* in the main text. Future studies could elucidate the nature of these resonances.

The density of states of a dihydrogen-monovacancy in Fig. S2d displays a peak near the Dirac point, which is superficially similar to the d*I*/d*V* acquired on a triangular defect in Fig. S1. However, the peak in Fig. S1 has a nontrivial dependence on V_g, so a more systematic study is required to understand the electronic structure of dihydrogen-monovacancies.

While our calculations indicate that a monohydrogen-monovacancy has a nonzero magnetic moment, we find that a dihydrogen-monovacancy does not possess a magnetic structure as the two hydrogen atoms pacify all dangling bonds of the vacancy. Similarly, hydrogen dimers do not have magnetic moments.

3. STM simulations at different voltage biases

DFT has difficulty obtaining correct energies for localized impurity states. The main text shows simulated STM images for hydrogen defect structures at $V_s = \pm 0.1$ Rydberg = ±1.36 V. Here in the Supplemental Material, we show additional simulated images of a monohydrogen-monovacancy and a dihydrogen-monovacancy in Fig. S3 and an ortho and a para dimer in Fig. S4. These simulations were performed for voltage biases closer to the Fermi energy E_F than the ±1.36 V images in the main text. The simulated images in Fig. S3 and S4 are qualitatively similar to the main text simulations, but the simulated dihydrogen-monovacancy in the main text better matches the experimental data than the Fig. S3 image.

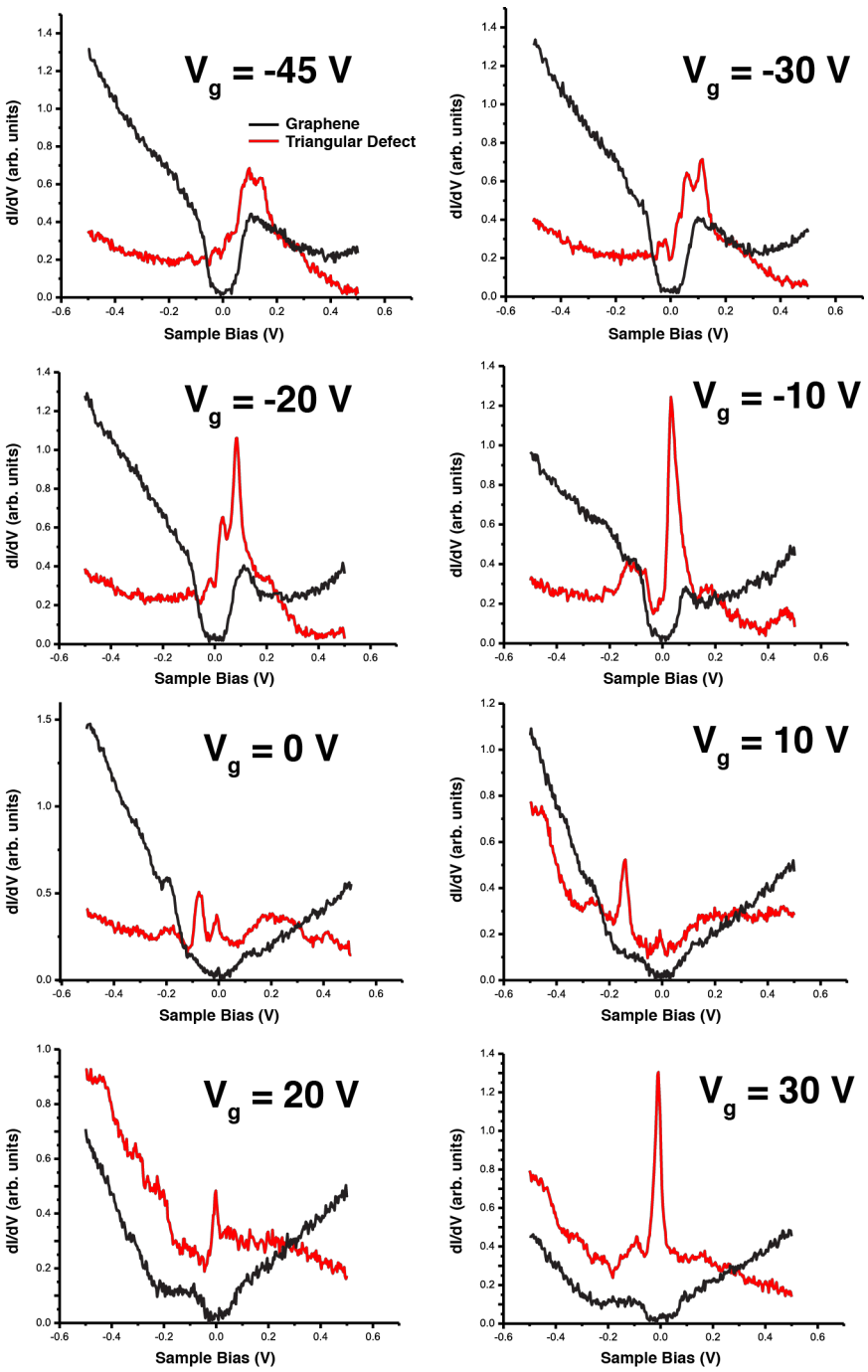

Figure S1. Gate-dependent d*I*/d*V* spectroscopy on a triangular defect. The black curves are d*I*/d*V* spectra acquired on bare graphene, while the red curves were obtained on the triangular defects.

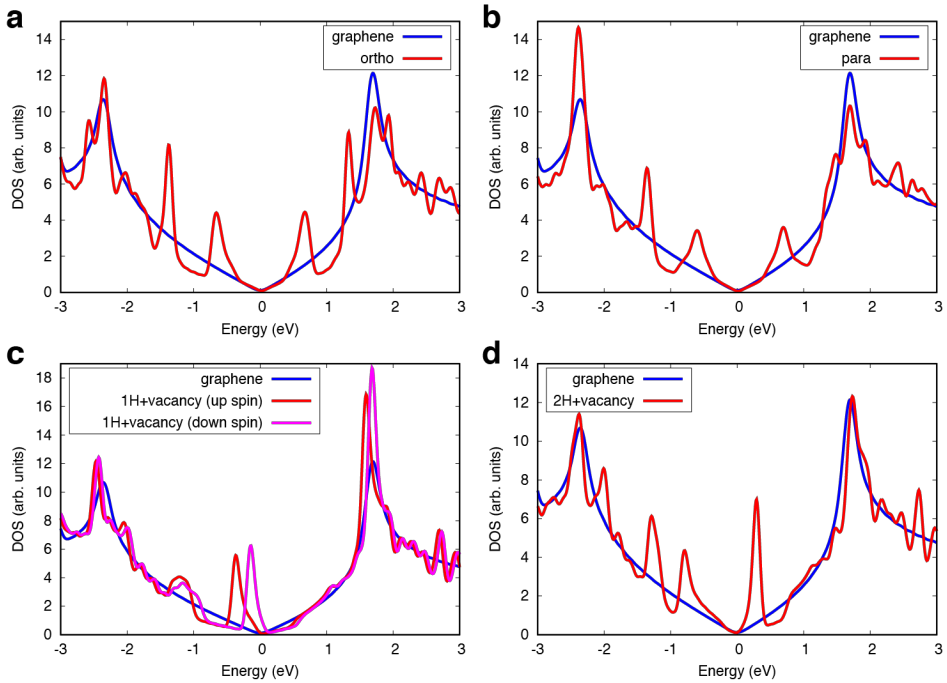

Figure S2. Density of states for hydrogen defect structures. Blue curves are DFT-calculated density of states for bare graphene, while red curves are calculated density of states for (**a**) an ortho dimer, (**b**) a para dimer, (**c**) a monohydrogen-monovacancy (spin up and spin down are shown separately), and (**d**) a dihydrogen-monovacancy.

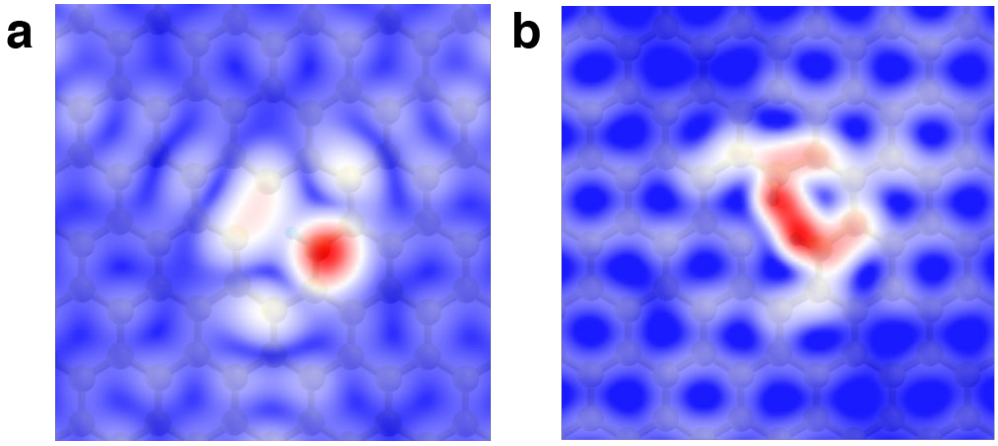

Figure S3. Additional STM simulations of hydrogen-vacancy complexes. (**a**) Simulated image of a monohydrogen-monovacancy at V_s = -0.4 V. (**b**) Same as **a** for a dihydrogen-monovacancy.

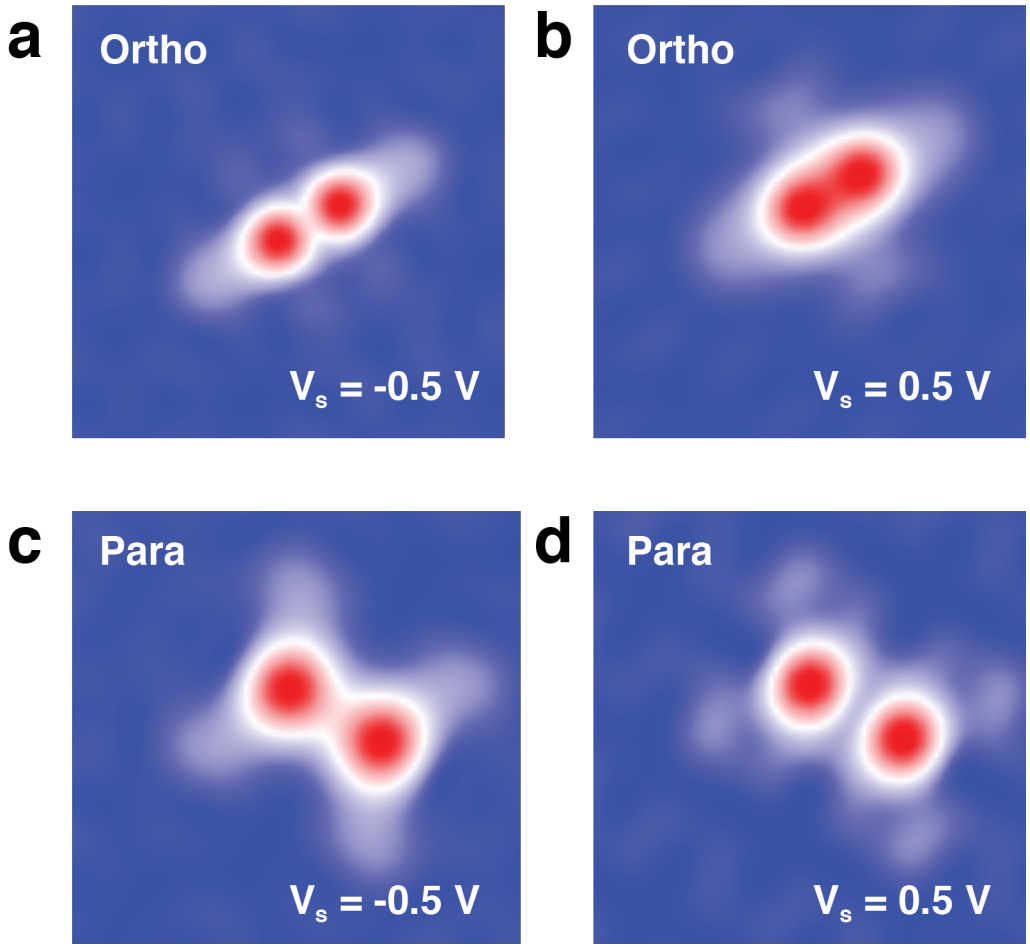

Figure S4. Additional STM simulations of hydrogen dimers. (**a**) Simulated image of an ortho dimer at V_s = -0.5 V. (**b**) Same as **a** for V_s = 0.5 V. (**c**) Simulated image of a para dimers at V_s = -0.5 V. (**d**) Same as **c** for V_s = 0.5 V.